arXiv:1606.00944v2 [cond-mat.stat-mech] 18 Apr 2017

Microcanonical Szilárd engines beyond the quasistatic regime

Thiago V. Acconcia[1,*] and Marcus V. S. Bonança[1,†]

[1] *Instituto de Física 'Gleb Wataghin', Universidade Estadual de Campinas, Rua Sérgio Buarque de Holanda, 777, 13083-859 Campinas, SP, Brazil*

(Dated: April 19, 2017)

We discuss the possibility of extracting energy from a single thermal bath using microcanonical Szilárd engines operating in finite time. This extends previous works on the subject which are restricted to the quasistatic regime. The feedback protocol is implemented based on linear response predictions of the excess work. It is claimed that the underlying mechanism leading to energy extraction does not violate Liouville's theorem and preserves ergodicity throughout the cycle. We illustrate our results with several examples including an exactly solvable model.

PACS numbers: 05.70.Ln, 82.60.Qr

I. INTRODUCTION

Over the last twenty years there has been an intense research activity on the interplay between information and thermodynamics. This field of investigation dates back to Maxwell who introduced a *gedanken* experiment where a being, the so-called Maxwell's demon, is able to violate the second law based on the knowledge acquired about the microscopic states of the system of interest [1–3]. This paradox was later on reformulated by Szilárd [4], who devised an engine able to extract energy from a single thermal bath. In Szilárd's setup, not only the information gathered by the demon is more easily quantified but also its role on the conversion of heat into work becomes more transparent. Hence it has become crucial to understand how thermodynamic entropy and information are related.

Major efforts on this direction have been made, for instance, by Brillouin, Landauer, Bennett and Penrose [5–8] who have discussed the energetic costs of measurement and measurement erasure. Along these lines, the demon operating the Szilárd engine needs a memory device to store the information gathered by him. To reset this memory at the end of the cyclic process, the demon has to dissipate an amount of energy that is generally greater than the extracted work. Hence the second law is rescued within this scenario by attributing an entropic cost for the measurement erasure. Besides the conceptual debate, several experimental setups have recently analysed these issues [9–12].

In the last decade, feedback controlled processes such as those performed by a Maxwell's demon have been incorporated into the frameworks of fluctuation theorems [13–19] and stochastic thermodynamics [20–24] leading to significant progress on the history of information in thermodynamics. More recently, the demon itself has been modeled as a physical system, yielding an antonomous formulation of the original paradox [25–31]. In this new point of view, a self-contained universe is composed of a device, the thermal reservoirs, a work source and an information reservoir. This composite system evolves autonomously and any effective feedback control arises from the interplay of the different subsystems.

In the present work, we focus on a particular kind of feedback control, namely, the microcanonical Szilárd engine [32, 33]. In this setup, the demon performs an energy measurement on a system initially equilibrated with a heat bath. The demon then acts according to the outcome of energy measurement keeping the system *isolated* from the reservoir. Effectively, one may think of a demon acting on a system initially prepared in a microcanonical ensemble. The examples available in the literature so far deal with the quasistatic regime, which means zero power extracted by the demon. Hence it is highly desirable to construct a microcanonical Szilárd engine operating in finite time.

In the quasistatic regime, the energy extraction is a consequence of an effective symmetry breaking [12, 34, 35]. Nevertheless, we show that it is also possible to extract energy in finite time without splitting the phase space in two or more disconnected regions. Moreover, we show that for certain protocols the work performed in finite time can be equal to the quasistatic work. These are essentially the basic ingredients we use to construct microcanonical Szilárd engines producing finite power.

The outline of the paper is as follows: in Sec. II we discuss which are the essential features of our construction of microcanonical Szilárd engines; in Sec. III, these features are illustrated with an exactly solvable model; an interpretation of our results in terms of phase space is given in Sec. IV; additional examples and final remarks are presented in Sec. V and VI, respectively.

II. MICROCANONICAL SZILÁRD ENGINES IN FINITE TIME

We shall start describing a general process performed on an arbitrary microcanonical Szilárd engine. Firstly, the system representing the engine is put in contact with a reservoir at temperature T. After its relaxation,

* thiagova@ifi.unicamp.br
† mbonanca@ifi.unicamp.br

the system is found in a Boltzmann-Gibbs distribution $\rho_{eq}(\Gamma,\lambda) = \exp(-\beta\mathcal{H}(\Gamma;\lambda))/\mathcal{Z}(\beta,\lambda)$, where Γ is a point in phase space, λ is an external control parameter, $\mathcal{H}$ is the system's Hamiltonian, $\beta = (k_B T)^{-1}$, with k_B being the Boltzmann constant. The quantity expressed by $\mathcal{Z}(\beta,\lambda_0)$ is the partition function of the system.

The engine is then decoupled from the heat bath and the demon measures its energy, causing the collapse of the initial Boltzmann-Gibbs distribution into a microcanonical one. After that, the engine will be driven by the demon in a two-stage process while it is kept isolated from the reservoir. We denote by step 1 the part of the cyclic process in which the system starts with a well-defined energy E_1 and the external parameter is driven from λ_1 to λ_2. This process takes a time interval τ_1 that has been carefully chosen by the demon based on the value of E_1. To complete the cycle, the external parameter is driven in the opposite direction, i.e., from λ_2 to λ_1. This step 2 takes a time interval τ_2 that is different from τ_1.

In step 1, the demon chooses a particular protocol and switching time τ_1 so that the average work performed is the *quasistatic* work W_{qs}. In other words, after several realizations of the cycle, the work performed along this part of the cyle is on average equal to the value obtained after a quasistatic switching from λ_1 to λ_2. Furthermore, this means that after step 1 the initial energy shell is basically mapped onto another energy shell. This phenomenon was already discussed elsewhere [36, 37] and a numerical evidence of it is presented in Fig. 1(a). We would like to stress that, despite of the two pronounced peaks of the energy distributions shown there, the average energy is exactly equal to the energy predicted by the adiabatic invariant (which is the volume enclosed by the energy shell).

In step 2, the demon chooses another particular protocol and switching time τ_2 to drive λ from λ_2 to λ_1. In this process, the average work W is equal to the negative of the quasistatic work W_{qs} obtained in step 1 plus the excess work W_{ex}. The protocol and switching time τ_2 are such that $W_{ex} < 0$ (see Fig. 2 and Sec. V for examples). Hence the net work that has been performed in the cycle is negative, meaning that energy was extracted. It is noteworthy that, in contrast to the corresponding quasistatic engines [32, 33], no ergodicity breaking is necessary, i.e., it is not necessary to split the phase space into disconnected regions.

In summary, our finite-time microcanonical Szilárd engine is based on the existence of finite-time protocols leading to $W = W_{qs}$ or $W_{ex} < 0$ according to the value of the switching time. It remains to be explained how it is possible to find such protocols and why (or more precisely for which class of systems) they yield such features. Based on extensive numerical investigation, we claim that several anharmonic oscillators of one degree of freedom share these properties (see Sec. V). In what follows, we take an analytically solvable example to show how to find the protocols we are interested in.

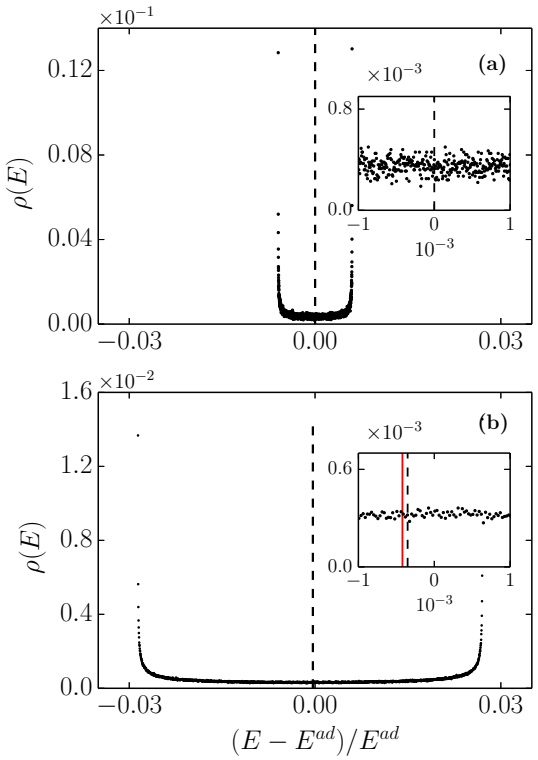

FIG. 1. (color online) Energy distribution after a finite-time driving of system (1) using the linear protocol $\lambda(t) = \lambda_0 + \delta\lambda(t-t_0)/\tau$ with $\delta\lambda/\lambda_0 = 0.1$. Vertical dashed lines represent the average energy for 10^6 initial conditions. The energy was rescaled in terms of the energy after the corresponding quasistatic protocol. (a) Energy distribution after a single linear switching such that $W_{ex} = 0$. (b) Energy distribution after a cyclic switching of λ in two linear steps, first, with $W_{ex} = 0$ and after with $W_{ex} < 0$. The continuous vertical red line corresponds to the linear response prediction.

III. EXACTLY SOLVABLE MODEL

We will consider in this section the following system

$$\mathcal{H}(t) = \epsilon^{-1}\, H_{HO}^2 = \frac{1}{\epsilon}\left[\frac{p^2}{2m} + \lambda(t)\frac{x^2}{2}\right]^2 , \qquad (1)$$

where H_{HO} is the harmonic oscillator Hamiltonian, ϵ is a constant and $\lambda(t)$ is the externally controlled parameter whose time-dependence is expressed in general by $\lambda(t) = \lambda_0 + \delta\lambda\, g(t)$, where $g(t)$ is such that $g(t_0) = 0$ and $g(t_f) = 1$, $\tau \equiv t_f - t_0$. The solutions of Hamilton's equations of are

$$x(t) = x(t_0)\cos(\omega t) + \frac{p(t_0)}{m\omega_0}\sin(\omega t) , \qquad (2a)$$

$$p(t) = p(t_0)\cos(\omega t) - m\omega_0 x(t_0)\sin(\omega t) , \qquad (2b)$$

where $\omega_0 = \sqrt{\lambda_0/m}$ and $\omega = 2\omega_0\sqrt{E/\epsilon}$ is the natural frequency of oscillations for an energy E. They describe an oscillatory motion with an energy-dependent angular

frequency and whose phase space is bounded as, for instance, a pendulum.

The thermodynamic work W performed when the external parameter λ is switched from λ_0 to $\lambda_f = \lambda_0 + \delta\lambda$ reads

$$W = \int_{t_0}^{t_f} dt\, \dot{\lambda}\, \overline{\frac{\partial \mathcal{H}}{\partial \lambda}}\,, \tag{3}$$

where $\overline{A}$ is the out-of-equilibrium average of the quantity A.

Restricting ourselves to processes in which $\delta\lambda/\lambda_0 \ll 1$ (but which are not necessarilly slow), we can apply linear response theory to relate the out-of-equilibrium average $\overline{\partial\mathcal{H}/\partial\lambda}$ to its corresponding relaxation function $\Psi_0(t)$ [38, 39]. For a system initially in a microcanonical equilibrium distribution whose energy is $E_0 = \mathcal{H}(t_0)$, $\Psi_0(t)$ is given by [40]

$$\Psi_0(t) = \frac{1}{Z(\lambda_0, E_0)} \frac{\partial}{\partial E_0} \left[Z(\lambda_0, E_0)(C(t) - \mathcal{C}) \right] \,, \tag{4}$$

where $Z(\lambda_0, E_0) = \int dx\, dp\, \delta(E_0 - \mathcal{H}(x, p; \lambda_0))$, $C(t) = \langle \partial\mathcal{H}(0)/\partial\lambda \; \partial\mathcal{H}(t)/\partial\lambda \rangle_0$ and $\mathcal{C}$ is the asymptotic value, for large t, of the correlation function $C(t)$ (for simply oscillatory functions, this has to be properly defined. See, for instance, Sec. 4.2.2 of [39]). We denote by $\langle A \rangle_0$ the microcanonical average of the observable A.

After some algebra linking Eq. (3) to the relaxation function (4) (see Appendix A), we obtain an expression for W given by the sum of two contributions. The first one can be identified with the quasistatic work along a equivalent quasistatic process and reads

$$W_{qs} = \delta\lambda \left\langle \frac{\partial \mathcal{H}}{\partial \lambda} \right\rangle_0 - \frac{(\delta\lambda)^2}{2} \tilde{\Psi}_0(0) \,, \tag{5}$$

where $\tilde{\Psi}_0 \equiv \Psi_0(0) - \chi_0^\infty$ with $\chi_0^\infty = \langle \partial^2\mathcal{H}/\partial\lambda^2 \rangle_0$.

It is worth notice that both terms *do not* depend on the protocol $g(t)$. Indeed, it can be verified that they are the first terms of the series expansion of the quasistatic work for $\delta\lambda/\lambda_0 \ll 1$.

The second contribution for the total work is a term that vanishes in the quasistatic limit and clearly depends on $g(t)$. Therefore, it is called excess work and reads [36],

$$W_{ex} = \frac{(\delta\lambda)^2}{2} \int_{t_0}^{t_f} dt \int_{t_0}^{t_f} dt'\, \Psi_0(t - t') \dot{g}(t) \dot{g}(t') \,. \tag{6}$$

In other words, $W_{ex} \equiv W - W_{qs}$ is the extra amount of energy the external agent has to pump into the system during a finite-time process.

The previous analysis about the linear response expression for W is very general and can now be applied to the system (1). The correlation function $C(t)$ can be calculated analytically from the previous expressions for $x(t)$ and $p(t)$ of (2) yielding the following relaxation function

$$\Psi_0(t) = \frac{E}{4\lambda_0^2} \left[3\cos(2\omega t) - 2\omega t \sin(2\omega t) \right] . \tag{7}$$

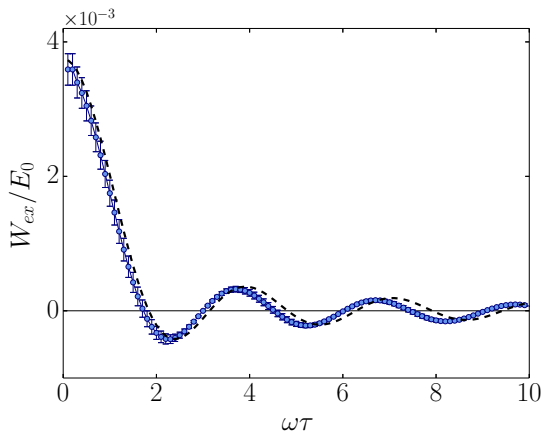

FIG. 2. (color online) Comparison between numerical results (blue circles) and linear response prediction (Eq. (8)) (dashed line) of W_{ex} as a function of the switching time τ for system (1). It was chosen the linear protocol $g(t) = (t - t_0)/\tau$ and $\delta\lambda/\lambda_0 = 0.1$. We used 10^6 initial conditions to calculate numerically the excess work for each τ.

Finally, we can calculate W_{ex} analytically for a given protocol $g(t)$ using Eq. (6). In particular, for the linear protocol $g(t) = (t - t_0)/\tau$ the result reads

$$W_{ex}(\tau) = \frac{E_0}{8} \left(\frac{\delta\lambda}{\lambda_0} \right)^2 \frac{\sin(\omega\tau)[(2\omega\tau)\cos(\omega\tau) + \sin(\omega\tau)]}{(\omega\tau)^2} . \tag{8}$$

The previous expression has several important features. As mentioned before, it goes to zero when we take the limit $\omega\tau \to \infty$. For large values of $\omega\tau$, we find that $W_{ex} \propto 1/\tau$, which can be related to the Sekimoto-Sasa relation presented in Refs.[41, 42]. The result of the last equation also reveals that W_{ex} can be null for *finite* values of τ. This happens either (i) when $\sin(\omega\tau)$ is zero, i.e., $\omega\tau = 2\pi k$, with k an integer; or (ii) when $\tan(\omega\tau)/2 = -\omega\tau$. It also predicts *negative* values of W_{ex} for specific ranges of τ. Figure 2 shows the comparison between Eq. (8) and numerical simulations using the linear protocol. Numerics were implemented using symplectic integrators [43].

The agreement between theoretical prediction for W_{ex} and the numerical calculation is very good. Although the theoretical prediction is restricted to weak driving, i.e., $\delta\lambda/\lambda_0 \ll 1$, it includes arbitrarily fast processes. Besides, Eq. (8) predicts the special switching times for which the excess work is either zero or negative. Additionally, we have investigated numerically the behavior of the excess work upto $\delta\lambda/\lambda_0 = 1.0$. Figure 3 shows that the linear response expression clearly deviates from the numerical calculations as $\delta\lambda/\lambda_0$ increases. However, it also shows that negative values of excess work are not restricted to our linear response regime.

In summary, it is possible to implement a microcanonical Szilárd engine driving system (1) with linear protocols as follows. In step 1, the control parameter is driven from

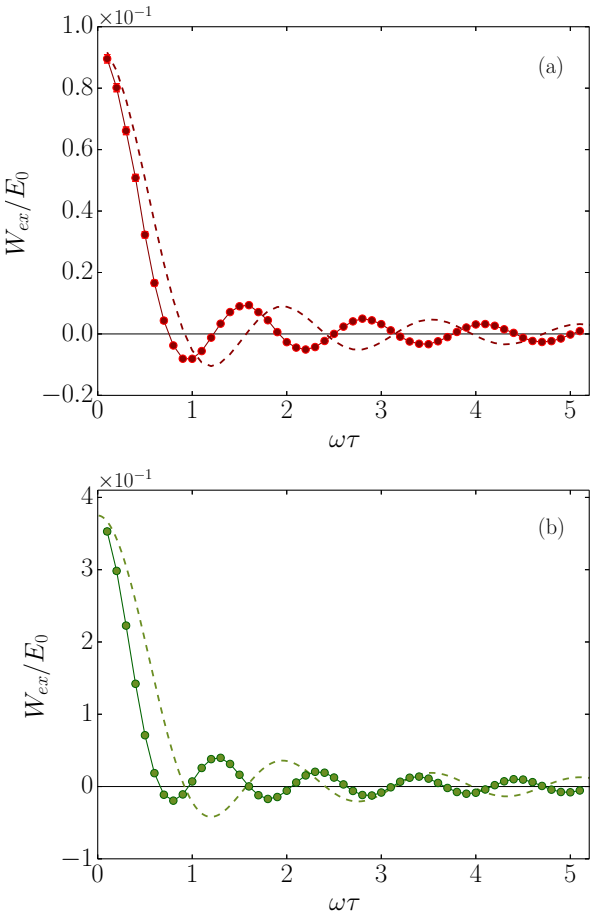

FIG. 3. (color online) Comparison between numerical calculations (circles) and linear response predictions (Eq. (8)) (dashed line) of W_{ex} as a function of the switching time τ for system (1). The driving was performed using the linear protocol $g(t) = (t-t_0)/\tau$ with (a) $\delta\lambda/\lambda_0 = 0.5$ and (b) $\delta\lambda/\lambda_0 = 1.0$. We used 10^6 initial conditions to calculate numerically the excess work for each τ.

$\lambda_0 + \delta\lambda$ to λ_0 in a time interval τ_1 yielding the first zero of W_{ex}. In step 2, another linear protocol drives λ back to λ_0 taking a time interval τ_2 such that $W_{ex} < 0$. Thus, the net work performed in the cycle is $W_{ex}(\tau_2)$. Since ω is a function of the energy, the duration of each protocol is chosen based on the information gathered by demon about the initial energy.

In contrast to the quasistatic regime, the finite-time driving of the system leads to different values of work after each single realization of the protocol. Hence we want to stress that our results are valid on average. Indeed, every time the demon starts a new cycle, the outcome of the energy measurement differs from the previous one. To obtain the curve in Fig. (2), the demon has then to sort his ensemble of trajectories by their initial energy values and take an average using only trajectories with essentially the same initial energy. Instead, if all trajectories are considered, the work performed in a cycle is on average equal to

$$\langle W_{cycle}\rangle = \frac{1}{\mathcal{Z}(\beta)}\int_0^\infty dE\; e^{-\beta E} Z(E)\; W_{ex}(E,\tau_2(E)) = -\frac{1}{16\beta}\left(\frac{\delta\lambda}{\lambda_0}\right)^2 |f(\omega\tau_2)|\;, \tag{9}$$

where $W_{ex}(\tau_2)$ is the value of the first minimum of Eq. (8), $f(\omega\tau) = \sin(\omega\tau)[2\omega\tau\cos(\omega\tau) + \sin(\omega\tau)]/(\omega\tau)^2$ and $Z(E)$ is the density of states. Since $\omega\tau_2 \approx 2.4$ does not depend on the energy, $f(\omega\tau_2) \approx -0.34$ can be taken outside the integral. It is worth mentioning that the demon can always find a suitable protocol yielding $W_{ex} < 0$ no matter the value of the energy measured.

IV. PHASE SPACE DYNAMICS

After presenting the linear response description of finite-time microcanonical Szilárd engines, we shall discuss the physical mechanism behind the energy extraction in our setup. The protocols we have discussed previously never split the phase space of the system in two or more disconnected parts [12, 34, 35]. Nevertheless, Figure 1 shows that, after a finite-time process, the energy distribution is essentially zero except for two particular values of energy, i.e., the system basically assumes either one or the other value of energy.

It is necessary to demand a bit more from the energy distribution in order to extract energy. The peak corresponding to the lower value of energy has to be higher otherwise W_{ex} never becomes negative. This is not possible in a harmonic oscillator as shown below. Its energy distribution after a finite-time driving also presents two pronounced peaks (see Fig. 6) but W_{ex} is always non-negative (see Eq. (12)). Our claim about why the anharmonic oscillators yield $W_{ex} < 0$ is based on the phase-space plots in Fig. 4 for the quartic oscillator of Eq. (13).

The initial energy shell is deformed along the momentum and coordinate directions when the system is driven quasistatically. Nevertheless, our numerical simulations indicate that the stretching and contraction directions rotate when an anharmonic oscillator is driven in finite time. Instead they remain fixed for the harmonic oscillator. In order to make the smaller value of energy more probable, the deformed curved must have a bigger portion of it tangential to the inner energy shell. This seems to be possible only when the stretching and contraction directions rotate in phase space.

A. Harmonic Oscillator

We briefly discuss now why the harmonic oscillator does not reproduce the behaviour we observe in Fig. 2.

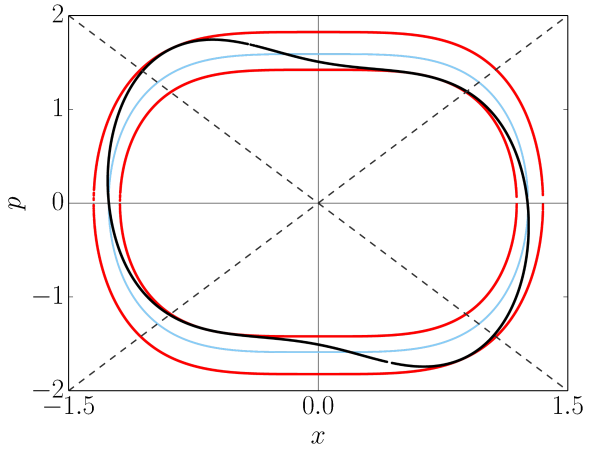

FIG. 4. (color online) Phase space distribution for the quartic oscillator. The black curve represents the deformed energy shell after a finite-time protocol yielding $W_{ex} < 0$. The outer and inner red (dark gray) curves are the energy shells corresponding, respectively, to the maximum and minimum values of the energy distribution in Fig. 1(b). The blue (light gray) curve corresponds to the energy shell obtained after a quasistatic driving.

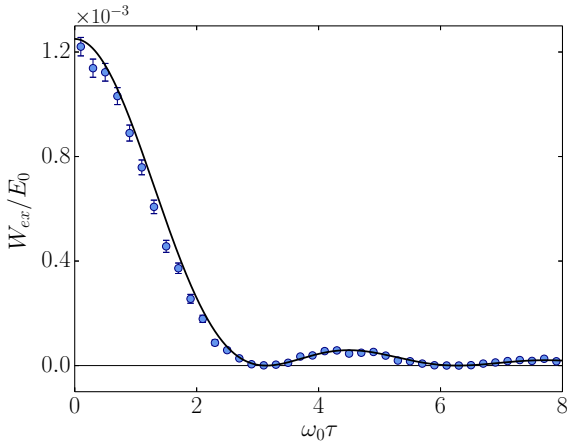

FIG. 5. (color online) Excess work as a function of the switching time for the harmonic oscillator. We compare numerical calculations (blue circles) and linear response prediction (solid line) when $g(t) = (t - t_0)/\tau$. We used 10^6 initial conditions for each switching time τ and fixed $\delta\lambda/\lambda_0 = 0.1$.

For the Hamiltonian,

$$H_{HO} = \frac{p^2}{2m} + \lambda(t)\frac{x^2}{2}\,, \tag{10}$$

the relaxation function can be obtain as described previously and it reads

$$\Psi_0(t) = \frac{E}{4\lambda_0^2}\cos(2\omega_0 t)\,. \tag{11}$$

Equations (6) and (11) then yield

$$\begin{aligned} W_{ex} &\propto \int_0^1 ds \int_0^1 du\ \cos(2\omega_0\tau(s-u))\dot{g}(s)\ \dot{g}(u) \\ &= \left(\int_0^1 ds\ \cos(2\omega_0\tau s)\ \dot{g}(s)\right)^2 + \\ &+ \left(\int_0^1 du\ \sin(2\omega_0\tau u)\ \dot{g}(u)\right)^2 . \end{aligned} \tag{12}$$

The excess work is therefore always positive for the harmonic oscillator. In other words, we could use this system to obtain zero excess work in finite time but it would be impossible to model a microcanonical Szilárd engine with it along the same lines presented in the paper. Figure 5 shows the comparison between numerical calculations and the linear response expression for the linear protocol.

Figure 6 shows the energy distribution of the harmonic oscillator after a linear switching of λ. Although it presents the same structure we find in anharmonic oscillators, it does not favor the lower value of energy and, consequently, it does not give rise to negative values of W_{ex}.

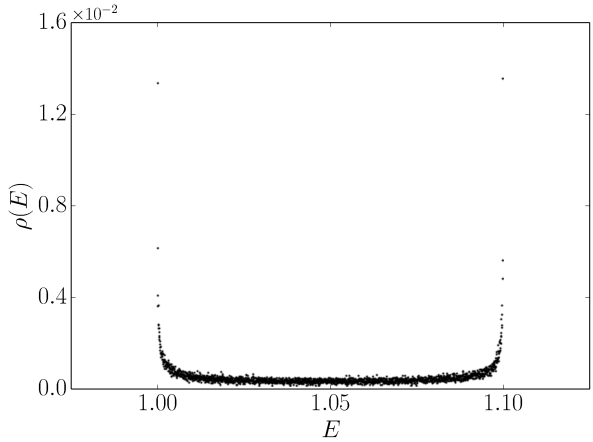

FIG. 6. (color online) Energy distribution of the harmonic oscillator (10) after a finite-time linear switching of λ. We set $\delta\lambda/\lambda_0 = 0.1$ and $\tau = 0.1\omega_0^{-1}$. We used 5×10^4 initial conditions.

Figure 7 shows the phase-space representation of the states leading to the energy distribution in Fig. 6. Since the switching time was chosen such that $W_{ex} > 0$, the initial set of phase-space points evolves to a curve that, although very close, is not a energy shell. The initial energy shell deforms along the momentum and coordinate axis even in finite time. This contrasts with what happens in anharmonic oscillators where the stretching and contraction directions rotate and coincide with the momentum and coordinate axis only in the quasistatic regime.

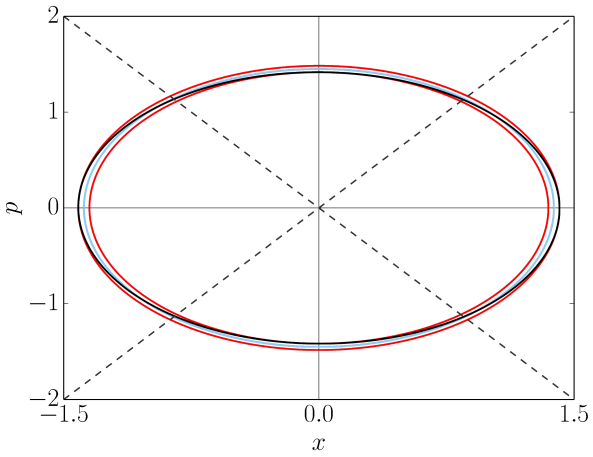

FIG. 7. (color online) Deformation of the initial energy shell of (10) after a finite-time driving of λ. The outer and inner red (dark gray) curves are energy shells corresponding, respectively, to the maximum and minimum values of the energy distribution in Fig. 6. The black curve represents the finite-time deformation of the initial energy shell after the linear protocol $g(t) = (t - t_0)/\tau$ with $\delta\lambda/\lambda_0 = 0.1$ and $\omega_0\tau = 0.1$. The blue (light gray) curve corresponds to the energy shell obtained after a quasistatic driving. We used 5×10^4 initial conditions for each curve.

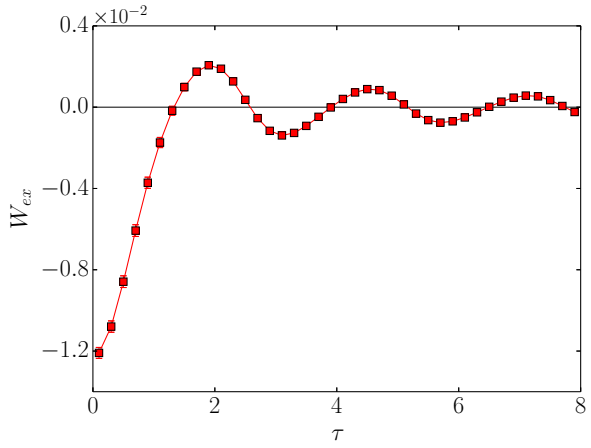

FIG. 8. (color online) Excess work as a function of the switching time for the system (13) using the linear protocol $g(t) = (t - t_0)/\tau$, $\delta\lambda/\lambda_0 = 0.1$ and 10^6 initial conditions for each value of τ.

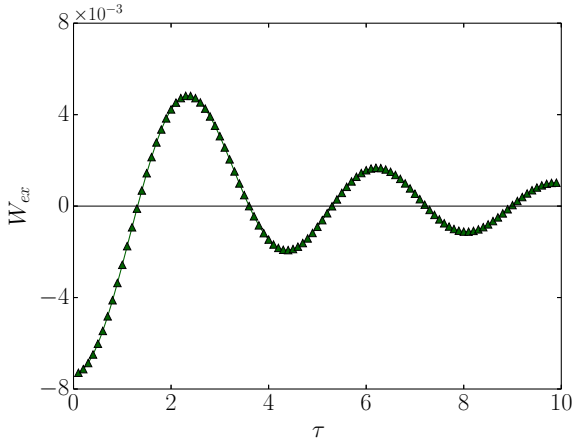

FIG. 9. (color online) Excess work as a function of the switching time for the system (14) using the linear protocol $g(t) = (t - t_0)/\tau$, $\delta\lambda/\lambda_0 = 0.1$ and 10^6 initial conditions for each value of τ.

V. OTHER EXAMPLES

The behavior of W_{ex} for the system (1) is typically found in other anharmonic oscillators. In what follows, we show numerical calculations of W_{ex} for a few examples: the quartic oscillator,

$$\mathcal{H}[\lambda(t)] = \frac{p^2}{2m} + \lambda(t)\frac{x^4}{2}\,, \tag{13}$$

the pendulum,

$$\mathcal{H}[\lambda(t)] = \frac{p^2}{2m} + 2\lambda(t)\sin^2\left(\frac{x}{2}\right)\,, \tag{14}$$

and the logarithmic oscillator,

$$\mathcal{H}[\lambda(t)] = \frac{p^2}{2m} + \lambda(t)\log\left(\frac{x^2+b^2}{b^2}\right)\,, \tag{15}$$

where b is a fixed parameter.

The corresponding excess work as a function of the switching time is presented in Figs. 8 to 10 for a linear switching of λ. We would like to highlight that the system (15) was used as an ideal Hamiltonian thermostat in [44]. We also present the energy distribution of the system (13) in Fig. 11 to stress the average negative work after the finite-time driving for the particular switching time $\tau = 0.3$.

VI. CONCLUDING REMARKS

In conclusion, we have shown how to construct finite-time microcanonical Szilárd engines for systems whose excess work presents finite-time zeros and negative values in non-cyclic processes. In contrast to previous examples available in the literature, these engines produce finite power on average. The cyclic process was obtained using a linear response approach which can be further explored to furnish the optimal protocols yielding the maximum energy extraction. Despite of the unexpected absence of ergodicity breaking, we have shown that it is still possible to extract energy due to special features of the energy distribution. This question deserves further investigation especially if one wants to extend the present results to systems with a larger number of degrees of freedom.

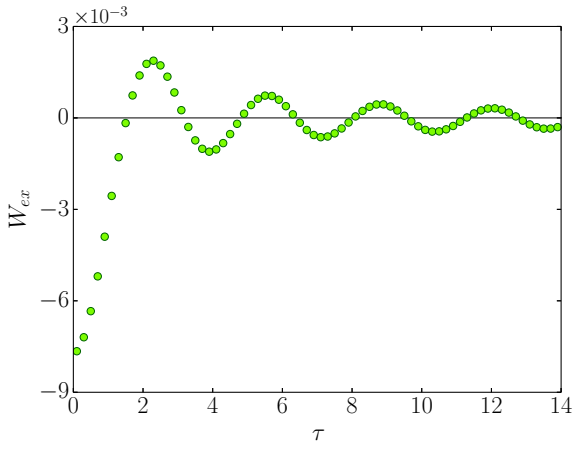

FIG. 10. (color online) Excess work as a function of the switching time for the system (15) using the linear protocol $g(t) = (t - t_0)/\tau$, $\delta\lambda/\lambda_0 = 0.1$ and 10^6 initial conditions for each value of τ.

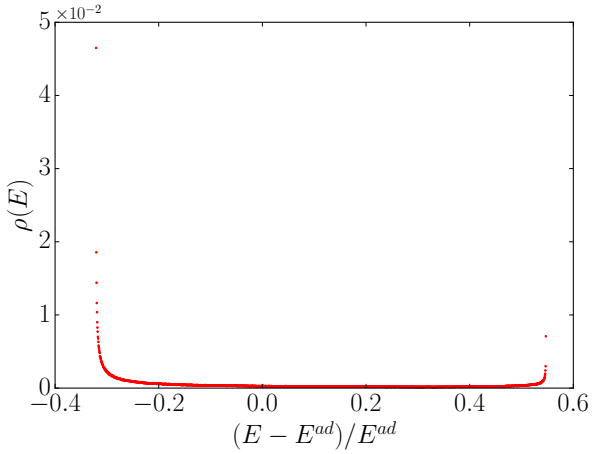

FIG. 11. (color online) Energy distribution after a finite-time driving of system (13) using a linear protocol $g(t) = (t-t_0)/\tau$, $\delta\lambda/\lambda_0 = 0.1$ and 10^6 initial conditions for each value of τ. The values of energy were rescaled by the corresponding value after a quasistatic driving.

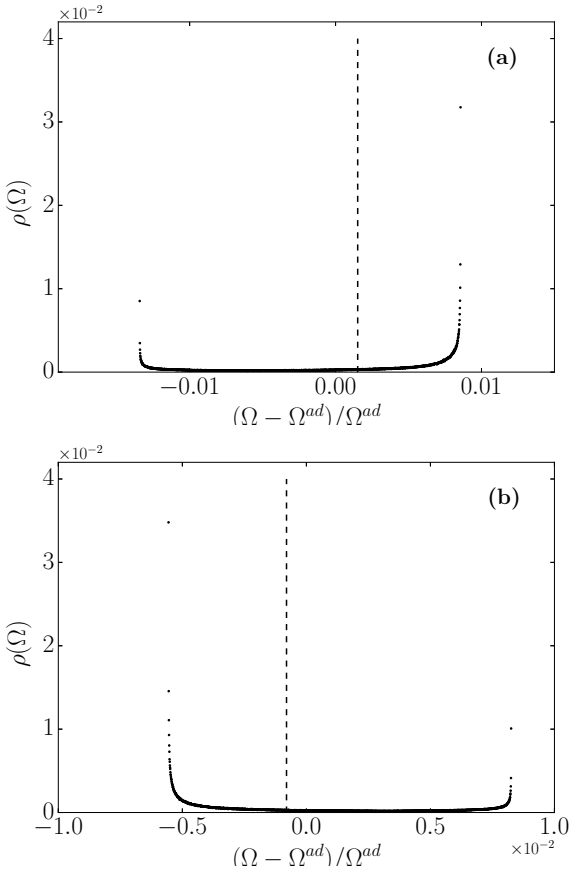

FIG. 12. (color online) Distribution of volumes Ω of energy shells obtained after a finite-time linear switching of λ in Hamiltonian (13) using switching times (a) $\tau = 1.6$ and (b) $\tau = 0.9$ (see Fig. 8). Since $\Omega = \int dqdp\,\Theta(E - H(q,p;\lambda)) \sim E^{3/4}$, its distribution is obtained from the distribution $\rho(E)$ of energies taking $\rho(E(\Omega))\,dE/d\Omega$. The values of Ω were rescaled by the value Ω^{ad} of the initial energy shell which is preserved in a quasistatic driving. The vertical dashed lines indicate the average value of Ω.

The energy extraction in Szilárd engines is usually attributed to the sudden reduction of phase space volume due to a symmetry breaking [12, 34, 35]. In the present case, although there is no such mechanism, we may have an reduction of phase space volume on average. Since the volume Ω enclosed by an energy shell is a monotonic increasing function of the energy E, there is a one-to-one mapping between Ω and E. Thus, from a energy distribution as Fig. 1, it is possible to obtained the corresponding distribution of Ω. Figure 12 shows that every time the average energy, after a finite-time driving, is smaller (greater) than the corresponding energy after an equivalent quasistatic driving, the average value of Ω is also smaller (greater) than the corresponding volume predicted by the adiabatic invariant. In this sense, we might connect the energy extraction to a reduction of phase space volume on average.

As a final remark, we should mention that the quantification of the information gathered my the demon in our examples does not seem as straightforward as in Ref. [33]. This analysis will be left for a future work.

ACKNOWLEDGMENTS

The authors acknowledge J. P. Pekola, P. Talkner, M. Campisi, S. Deffner and W.H. Zurek for enriching discussions. We especially thank É. Roldán for the careful analysis of the manuscript and inspiring discussions. T.A. acknowledges support from 'Gleb Wataghin' Physics Institute (Brazil) and CAPES (Brazil), Grant No. 1504869. M.B. acknowledges financial support from Unicamp/FAEPEX (Brazil), Grant No. 0031/15 and

FAPESP (Brazil), Grant No. 2016/01660-2.

Appendix A: Excess work within linear response theory

In this appendix we derive the linear response expression for excess and quasistatic work. In the inclusive picture, the thermodynamic work produced during a finite-time driving of a control parameter λ is given by (3). Assuming that $|\delta\lambda g(t)/\lambda_0| \ll 1$ for $t_0 \leq t \leq t_f$, linear response theory provides the following relation between the out-of-equilibrium average and its corresponding response function $\phi_0(t)$ [38]

$$\overline{\frac{\partial \mathcal{H}}{\partial \lambda}}(t) = \left\langle \frac{\partial \mathcal{H}}{\partial \lambda} \right\rangle_0 + \chi_0^\infty \delta\lambda g(t) - \delta\lambda \int_{t_0}^{t} ds\, \phi_0(t-s)\, g(s), \tag{A1}$$

where $\langle\cdot\rangle_0$ denotes the average on the initial microcanonical ensemble and the subscript refers to the value λ_0. The second term in the right-hand side of Eq. (A1) describes the *instantaneous* response, which is due to $\partial\mathcal{H}/\partial\lambda$ being a function of the external control λ. In particular, we have

$$\chi_0^\infty = \left\langle \frac{\partial^2 \mathcal{H}}{\partial \lambda^2} \right\rangle_0 . \tag{A2}$$

The second term describes the *delayed* response. It is convenient to express it in terms of the *relaxation* function as $\phi_0(t) = -d\Psi_0(t)/dt$. Thus, integrating by parts Eq. (A1) we find

$$\overline{\frac{\partial \mathcal{H}}{\partial \lambda}}(t) = \left\langle \frac{\partial \mathcal{H}}{\partial \lambda} \right\rangle_0 - \delta\lambda \tilde{\Psi}_0(0) g(t) + \delta\lambda \int_0^{t-t_0} du\, \Psi_0(u) \frac{dg}{dt'}\bigg|_{t'=t-u} \tag{A3}$$

where $\tilde{\Psi}_0 \equiv \Psi_0(0) - \chi_0^\infty$. Finally, substituting Eq. (A3) in expression (3), we obtain

$$W = \delta\lambda \left\langle \frac{\partial \mathcal{H}}{\partial \lambda} \right\rangle_0 - \frac{(\delta\lambda)^2}{2} \tilde{\Psi}_0(0) + (\delta\lambda)^2 \int_{t_0}^{t_f} dt\, \frac{dg}{dt} \int_{t_0}^{t} dt'\, \Psi_0(t-t') \frac{dg}{dt'}\,, \tag{A4}$$

where the following boundary conditions, $g(t_0) = 0$ and $g(t_f) = 1$, were used. The first two terms of the previous expression *do not* depend on the protocol $g(t)$. Indeed, it can be verified that they are the first terms of the series expansion of the quasistatic work for $\delta\lambda/\lambda_0 \ll 1$ given in (5). The last term clearly depends on $g(t)$ and therefore represents the *excess* work given by (6).

[1] J. Maxwell, *Theory of Heat*, Text-books of science (Longmans, 1871).
[2] H. Leff and A. Rex, *Maxwell's Demon: Entropy, Information, Computing*, Princeton Legacy Library (Princeton University Press, 2014).
[3] K. Maruyama, F. Nori, and V. Vedral, Rev. Mod. Phys. **81**, 1 (2009).
[4] L. Szilárd, Z. Phys. **53**, 840 (1929).
[5] L. Brillouin, J. Appl. Phys. **22**, 334 (1951).
[6] R. Landauer, Phys. Today **44(5)**, 23 (1991).
[7] C. Bennett, Int. J. Theor. Phys. **21**, 905 (1982).
[8] O. Penrose, *Foundations of Statistical Mechanics: A Deductive Treatment* (Dover Publications, 2014).
[9] S. Toyabe, T. Sagawa, M. Ueda, E. Muneyuki, and M. Sano, Nature Phys. **6**, 988 (2010).
[10] A. Berut, A. Arakelyan, A. Petrosyan, S. Ciliberto, R. Dillenschneider, and E. Lutz, Nature **483**, 187 (2011).
[11] J. Koski, V. Maisi, T. Sagawa, and J. P. Pekola, Phys. Rev. Lett. **113**, 030601 (2014).
[12] E. Roldán, I. A. Martínez, J. M. R. Parrondo, and D. Petrov, Nature Phys. **10**, 457 (2014).
[13] T. Sagawa and M. Ueda, Phys. Rev. Lett. **100**, 080403 (2008).
[14] T. Sagawa and M. Ueda, Phys. Rev. Lett. **102**, 250602 (2009).
[15] T. Sagawa and M. Ueda, Phys. Rev. Lett. **104**, 090602 (2010).
[16] J. Horowitz and S. Vaikuntanathan, Phys. Rev. E **82**, 061120 (2010).
[17] M. Ponmurugan, Phys. Rev. E **82**, 031129 (2010).
[18] T. Sagawa and M. Ueda, Phys. Rev. E **85**, 021104 (2012).
[19] T. Sagawa and M. Ueda, Phys. Rev. Lett. **109**, 180602 (2012).
[20] M. Esposito and C. V. den Broeck, Europhys. Lett. **95**, 40004 (2011).
[21] D. Abreu and U. Seifert, Europhys. Lett. **94**, 10001 (2011).
[22] P. Strasberg, G. Schaller, T. Brandes, and M. Esposito, Phys. Rev. Lett. **110**, 040601 (2013).
[23] A. Barato and U. Seifert, Phys. Rev. Lett. **112**, 090601 (2014).
[24] A. Barato and U. Seifert, Phys. Rev. E **90**, 042150 (2014).
[25] D. Mandal and C. Jarzynski, Proc. Natl. Acad. Sci. USA **109**, 11641 (2012).
[26] A. Barato and U. Seifert, Europhys. Lett. **101**, 60001 (2013).
[27] S. Deffner and C. Jarzynski, Phys. Rev. X **3**, 041003 (2013).
[28] S. Deffner, Phys. Rev. E **88**, 062128 (2013).
[29] Z. Lu, D. Mandal, and C. Jarzynski, Phys. Today **67(8)**, 60 (2014).
[30] J. V. Koski and J. P. Pekola, Comptes Rendus Physique **17**, 1130 (2016).
[31] A. Kutvonen, J. Koski, and T. Ala-Nissila, Scientific Reports **6**, 21126 (2016).
[32] R. Marathe and J. M. R. Parrondo, Phys. Rev. Lett. **104**, 245704 (2010).
[33] S. Vaikuntanathan and C. Jarzynski, Phys. Rev. E **83**, 061120 (2011).
[34] J. M. R. Parrondo, Chaos **11**, 725 (2001).

[35] J. M. R. Parrondo and L. Granger, Eur. Phys. J. Special Topics **224**, 865 (2015).
[36] T. V. Acconcia and M. V. S. Bonança, Phys. Rev. E **91**, 042141 (2015).
[37] T. V. Acconcia, M. V. S. Bonança, and S. Deffner, Phys. Rev. E **92**, 042148 (2015).
[38] R. Kubo, J. Phys. Soc. Jpn. **12**, 570 (1957).
[39] R. Kubo, M. Toda, and N. Hashitsume, *Statistical Physics II - Nonequilibrium Statistical Mechanics* (Springer-Verlag, Berlin, 1985).
[40] M. V. S. Bonança, Phys. Rev. E **85**, 031122 (2012).
[41] K. Sekimoto and S. i. Sasa, Journal of the Physical Society of Japan **66**, 3326 (1997).
[42] I. A. Martinez, E. Roldan, L. Dinis, and R. A. Rica, Soft Matter **13**, 22 (2017).
[43] P. J. Channel and C. Scovel, Nonlinearity **3**, 231 (1990).
[44] M. Campisi, F. Zhan, P. Talkner, and P. Hanggi, Phys. Rev. Lett. **108**, 250601 (2012).